The Gold-rich Indide $Eu_5Au_{17.7}In_{4.3}$ and its Relation with the Structures of $SrAu_{4.76}In_{1.24}$ and $BaLi_4$

Ihor Muts[a,b], Ute Ch. Rodewald[a], Vasyl' I. Zaremba[b], Orest Pavlosyuk[b], and Rainer Pöttgen[a]

[a] Institut für Anorganische und Analytische Chemie, Universität Münster, Corrensstraße 30, 48149 Münster, Germany
[b] Inorganic Chemistry Department, Ivan Franko National University of Lviv, Kyryla and Mephodiya Street 6, 79005 Lviv, Ukraine

Reprint requests to R. Pöttgen. E-mail: pottgen@uni-muenster.de

The gold-rich indide $Eu_5Au_{17.7}In_{4.3}$ was synthesized from the elements in a sealed tantalum ampoule that was heated in a high-frequency furnace. $Eu_5Au_{17.7}In_{4.3}$ crystallizes with a new monoclinic structure type: $C2/m$, $a = 902.7(2)$, $b = 722.8(3)$, $c = 1734.1(4)$ pm, $\beta = 94.31(3)°$, $wR2 = 0.0907$, 2640 F^2 values and 74 variables. $Eu_5Au_{17.7}In_{4.3}$ has a pronounced gold substructure with Au–Au distances ranging from 278 to 300 pm. The striking structural motifs in the gold substructure are networks of Au_6 hexagons and discrete units of corner- and edge-sharing Au_4 tetrahedra. $Eu_5Au_{17.70}In_{4.30}$ exhibits a small homogeneity range with In/Au mixing on two Wyckoff sites. Geometrically, the $Eu_5Au_{17.7}In_{4.3}$ structure can be explained as an intergrowth variant of slightly distorted $SrAu_{4.76}In_{1.24}$- and $BaLi_4$-related slabs. The europium coordination in the $BaLi_4$ slabs is similar to binary $EuAu_2$.

Key words: Intermetallics, Europium, Indide, Gold Clusters

Introduction

The Eu–Au-*X* (*X* = Al, Ga, In, Tl, Si, Ge, Sn, Pb, P, As, Sb, Bi) systems have intensively been studied in the last twenty years with respect to phase formation and physical properties. The simplest composition, observed in almost all Eu–Au-*X* phase diagrams, concerns the equiatomic compounds Eu*AuX*. The crystal chemical details and the physical properties of these compounds are summarized in a review article [1]. The structural chemistry and the magnetic properties are goverened by a stable $4f^7$ Eu^{II} ground state and in some cases additionally by Au–Au d^{10}-d^{10} interactions or even by extended Au–Au bonding. To give some examples, secondary Au–Au interactions are the driving force for superstructure formation of EuAuGe (316 pm) [2] and EuAuSn (334 – 335 pm) [3], while Au–Au zig-zag chains (279 pm) occur in $EuAu_3In_3$ [4].

Most of the divalent europium compounds show magnetic ordering at low temperature, *e. g.* 5.8 K for $Eu_2Au_2Sn_5$ [5] or 21 K for EuAuIn [6]. Also $EuAu_2Si_2$ [7] with the $ThCr_2Si_2$-type structure contains stable divalent europium, but the systems tends to valence instabilities in the solid solution $Eu(Pd_{1-x}Au_x)_2Si_2$ [8, 9], similar to $EuPd_{1-x}Au_xAs$ [10].

The Eu–Au-*X* system with the largest number of ternary phases concerns *X* = In. The structures of equiatomic EuAuIn [6], $Eu_2Au_3In_4$ [11] and $EuAuIn_2$ [12] are built up from complex three-dimensional gold indium polyanionic networks in which the europium atoms fill larger cavities. The polyanionic networks show strong covalent Au–In besides In–In bonding in the indium-richer phases $Eu_2Au_3In_4$ and $EuAuIn_2$. So far, Au–Au bonding was only observed within the zig-zag chains of $EuAu_3In_3$ [4]. Since Eu^{2+} (112 pm) and Sr^{2+} (127 pm) have comparable ionic radii [13], and keeping the peculiar crystal structures of the gold-rich phases $SrAu_{4.76}In_{1.24}$ [14] and $Sr_5Au_{13.5}In_{8.5}$ [15] in mind, we were interested also in the gold-rich part of the Eu–Au-In system. Herein we report on the synthesis and structure of the indide $Eu_5Au_{17.7}In_{4.3}$, which crystallizes with its own structure type, but shows distinct similarities with the $SrAu_{4.76}In_{1.24}$ [14] structure.

Experimental Section

Synthesis

Starting materials for the syntheses of $Eu_5Au_{17.7}In_{4.3}$ were ingots of sublimed europium (Johnson Matthey), pieces of a gold bar (Heraeus), and indium ingots (Johnson Matthey), all with stated purities better than 99.9 %. The air- and moisture-sensitive europium ingots were kept under argon prior to the reaction. The argon was purified before with titanium sponge (870 K), silica gel and molecular sieves. The elements were weighed in the atomic ratio 1 : 4 : 1 and arc-welded [16] in a small tantalum ampoule. The tantalum tube was subsequently placed in the water-cooled sample chamber of an induction furnace [17] (Hüttinger Elektronik, Freiburg, Germany, Typ TIG 2.5/300) under flowing argon and first annealed at 1500 K for about one minute. Finally, the sample was cooled to 900 K within four hours and kept at that temperature for another 4 h, followed by switching off the power supply. The temperature was controlled by a Sensor Therm Methis MS09 pyrometer with an accuracy of ±30 K. No reaction with the crucible materials was evident. The compact and polycrystalline sample is stable in air for weeks. Small single-crystals exhibit metallic luster while ground powders are light grey.

EDX data

The $Eu_5Au_{17.7}In_{4.3}$ crystal studied on the diffractometer was investigated by semiquantitative EDX analyses by use of a Zeiss EVO MA10 scanning electron microscope (variable pressure mode) with EuF_3, Au, and InAs as standards. The experimentally observed composition (17 ± 2 at.-% Eu : 67 ± 2 at.-% Au : 16 ± 2 at.-% In) was close to the one (18.5 : 65.6 : 15.9) refined from the single-crystal diffraction data. No impurity elements were found.

X–Ray diffraction

The polycrystalline $Eu_5Au_{17.7}In_{4.3}$ sample was characterized by a Guinier powder pattern using $CuK\alpha_1$ radiation and α-quartz (a = 491.30 and c = 540.46 pm) as the internal standard. The Guinier camera was equipped with an imaging plate detector, coupled with a Fujifilm BAS-1800 readout system. The monoclinic lattice parameters (Table 1) were refined from the Guinier powder data with a standard least-squares routine. The correct assignment of the *hkl* indices was ensured by an intensity calculation [18] using the atomic positions from the structure refinement.

Small block-shaped single-crystals of $Eu_5Au_{17.7}In_{4.3}$ were selected from the mechanically crushed sample prepared in the high-frequency furnace. The crystals were glued to small quartz fibers using bees wax, and their quality was tested by Laue photographs on a Buerger camera (white Mo radiation). Intensity data of a good-quality crystal were col-

Table 1. Crystal data and structure refinement for $Eu_5Au_{17.70(3)}In_{4.30(3)}$; space group $C2/m$; $Z = 2$.

Unit cell dimensions (Guinier powder data)	
a, pm	902.7(2)
b, pm	722.8(3)
c, pm	1734.1(4)
β, deg	94.31(3)°
Cell volume V, nm^3	1.1283
Molar mass, g mol^{-1}	4740.24
Calculated density, g cm^{-3}	13.95
Absorption coefficient, mm^{-1}	132.5
$F(000)$, e	3848
Crystal size, μm^3	$10 \times 30 \times 60$
Transm. ratio (max / min)	0.463 / 0.074
θ range, deg	$2-35$
Range in *hkl*	$\pm14, \pm11, \pm27$
Total no. reflections	9901
Independent reflections / R_{int}	2640 / 0.1077
Reflections with $I \geq 2\sigma(I)$ / R_σ	1451 / 0.0772
Data / parameters	2640 / 74
$R1$ / $wR2$ for $I \geq 2\sigma(I)$	0.0418 / 0.0733
$R1$ / $wR2$ for all data	0.1091 / 0.0907
Goodness-of-fit on F^2	0.966
Extinction coefficient	0.000107(8)
Largest diff. peak /hole, e Å^{-3}	3.77 / -4.10

lected at r. t. on a four-circle diffractometer (CAD4) with graphite-monochromatized $MoK\alpha$ radiation and a scintillation counter with pulse height discrimination. Scans were taken in the $\omega/2\theta$ mode. A numerical absorption correction was applied to the data set. All relevant details concerning the data collection and evaluation are listed in Table 1.

Structure determination and refinement

The diffractometer data set showed a *C*-centered monoclinic lattice and no further systematic extinctions, leading to the possible space groups $C2$, Cm, and $C2/m$, of which the centrosymmetric group was found to be correct during structure refinement. The starting atomic parameters were determined *via* direct methods with SHELXS-97 [19], and the structure was refined using SHELXL-97 [20] (full-matrix least-squares on F^2) with anisotropic atomic displacement parameters for all atoms. During the refinement procedure, two sites could not reliably be assigned to gold or indium, indicating Au/In mixing, similar to the recently reported structures of $SrAu_{4.76}In_{1.24}$ [14] and $Sr_5Au_{13.5}In_{8.5}$ [15]. In the subsequent cycles, the Au/In mixing was refined as a least-squares variable, leading to the composition $Eu_5Au_{17.7}In_{4.3}$ for the investigated crystal. All other sites were fully occupied within two standard deviations. The final difference Fourier synthesis was flat (Table 1). The positional parameters and interatomic distances are listed in Tables 2 and 3.

Further details of the crystal structure investigation may be obtained from Fachinformationszentrum Karlsruhe, 76344 Eggenstein-Leopoldshafen, Germany (fax: +49-7247-

Atom	Wyckoff site	Occupancy	x	y	z	U_{eq}
Eu1	4*i*	100	0.4073(1)	0	0.24911(9)	103(2)
Eu2	2*a*	100	0	0	0	105(4)
Eu3	4*i*	100	0.7816(1)	0	0.50060(8)	107(2)
Au1	8*j*	100	0.32024(7)	0.1931(1)	0.07606(4)	119(1)
Au2	8*j*	100	0.08837(8)	0.1928(1)	0.17261(5)	124(1)
Au3	8*j*	100	0.48351(7)	0.1981(1)	0.41964(4)	108(1)
Au4	8*j*	100	0.22350(7)	0.3058(1)	0.32681(4)	125(1)
Au5/In3	4*i*	58(1)/42(1)	0.3119(1)	1/2	0.19095(9)	152(4)
In1	4*i*	100	0.0273(2)	0	0.3198(1)	129(4)
In2/Au6	4*i*	70(1)/30(1)	0.6045(2)	0	0.0640(1)	142(5)

Table 2. Atomic coordinates and isotropic displacement parameters (pm^2) of Eu$_5$Au$_{17.70(3)}$In$_{4.30(3)}$. U_{eq} is defined as one third of the trace of the orthogonalized U_{ij} tensor.

Crystal chemistry of Eu$_5$Au$_{17.7}$In$_{4.3}$

The gold-rich indide Eu$_5$Au$_{17.7}$In$_{4.3}$ crystallizes with a new monoclinic structure type, space group $C2/m$, Pearson code *mS*54. The structure contains

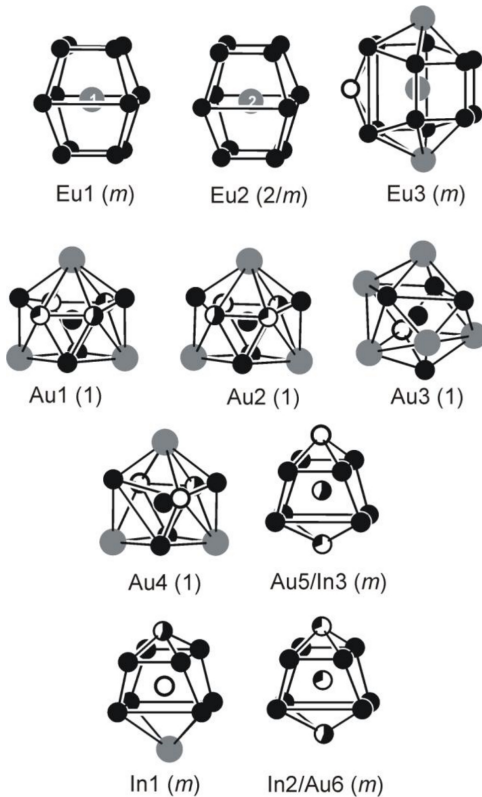Fig. 1. Coordination polyhedra in the structure of Eu$_5$Au$_{17.7}$In$_{4.3}$. Europium, gold and indium atoms are drawn as medium grey, black filled, and open circles, respectively. Mixed-occupied sites are emphasized by segments. The site symmetries are indicated.

Table 3. Interatomic distances (pm), calculated with the powder lattice parameters of Eu$_5$Au$_{17.70(3)}$In$_{4.30(3)}$. Standard deviations are all equal or less than 0.2 pm.

Atom				Atom			
Eu1:	2	Au2	311.2	Au3:	1	Au3	278.0
	2	Au4	312.9		1	Au4	279.5
	2	Au3	331.1		1	In1	283.2
	2	Au1	334.9		1	Au4	285.3
	2	Au4	337.0		1	Au3	286.4
	2	Au2	337.9		1	Eu3	319.2
Eu2:	4	Au1	310.1		1	Eu3	323.1
	4	Au2	334.3		1	Eu3	327.0
	4	Au1	338.7		1	Eu3	327.6
Eu3:	2	Au3	319.2		1	Eu1	331.1
	2	Au3	323.1	Au4:	1	Au3	279.5
	2	Au3	327.0		1	Au4	280.7
	2	Au3	327.6		1	In1	282.9
	2	Au4	333.0		1	Au3	285.3
	1	In1	344.5		1	Au5/In3	290.5
	2	Eu3	365.8		1	Au2	296.9
Au1:	1	Au2	277.7		1	In1	309.1
	1	Au1	279.1		1	Eu1	312.9
	1	In2/Au6	292.6		1	Eu3	333.0
	1	In2/Au6	294.2		1	Eu1	337.0
	1	In2/Au6	294.9	Au5/In3:	1	In2/Au6	278.1
	1	Au2	295.5		1	In1	285.0
	1	Au1	295.5		2	Au2	289.7
	1	Au5/In3	298.7		2	Au4	290.5
	1	Eu2	310.1		2	Au1	298.7
	1	Eu1	334.9		2	Au2	300.1
	1	Eu2	338.7	In2/Au6:	1	Au5/In3	278.1
Au2:	1	Au1	277.7		1	In2/Au6	280.3
	1	Au2	278.7		2	Au2	292.2
	1	Au5/In3	289.7		2	Au1	292.6
	1	In2/Au6	292.2		2	Au1	294.2
	1	Au1	295.5		2	Au1	294.9
	1	Au4	296.9	In1:	2	Au4	282.9
	1	In1	299.5		2	Au3	283.2
	1	Au5/In3	300.1		1	Au5/In3	285.0
	1	Eu1	311.3		2	Au2	299.5
	1	Eu2	334.3		2	Au4	309.1
	1	Eu1	337.9		1	Eu3	344.5

ten crystallographically independent sites with the Wyckoff sequence $ai^5 j^4$. The corresponding coordination polyhedra are presented in Fig. 1. The Eu1 and Eu2 atoms have twelve gold atoms in their quite similar coordination shell; however, they have different
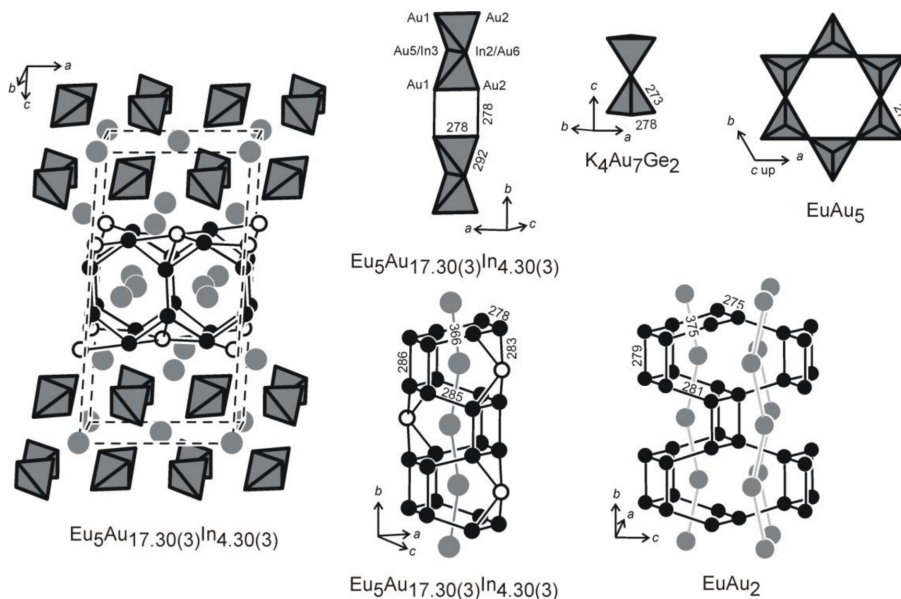
Fig. 2. Left: View of the Eu$_5$Au$_{17.7}$In$_{4.3}$ structure approximately along the *b* axis. Europium, gold and indium atoms are drawn as medium grey, black filled, and open circles, respectively. Part of the gold indium network and the gold tetrahedra are emphasized. Tetrahedral units in K$_4$Au$_7$Ge$_2$ [23] and EuAu$_5$ [23] are drawn for comparison (top). The europium coordination within the BaLi$_4$-related slab (see Fig. 3) is compared to binary EuAu$_2$ [22, 23].

site symmetry. The Eu–Au distances range from 310 to 339 pm, close to the sum of the covalent radii [13] of 319 pm. Also in EuAuIn [6] (317 – 334 pm), EuAuIn$_2$ [12] (317 – 332 pm), Eu$_2$Au$_3$In$_4$ [11] (305 – 351 pm), and EuAu$_3$In$_3$ [4] (334 – 338 pm) the europium sites have gold atoms as closest neighbors, since the Pauling electronegativity [13] of gold (2.54) is significantly higher than that of indium (1.78). The Eu1 (478 pm Eu1–Eu3) and Eu2 (546 pm Eu2–Eu1) atoms have no close Eu–Eu contacts. The corresponding distances are significantly longer than in the structure of *bcc* europium (397 pm Eu–Eu) [21]. The Eu3 atoms have a slightly higher coordination number with twelve gold, one indium, and two europium atoms in their coordination shell. The twelve gold neigbors form a distorted hexagonal prism which is somehow opened at the side where the indium atom is coordinating. The two europium neigbors are capping the slightly distorted Au$_6$ hexagons, leading to –Eu3–Eu3–Eu3– chains. In Fig. 2 we have outlined three successive Eu3 polyhedra, which are condensed *via* common Au$_6$ hexagons. This cutout of the Eu$_5$-Au$_{17.7}$In$_{4.3}$ structure is almost similar to binary EuAu$_2$ [22, 23] with an orthorhombic KHg$_2$-type structure and with similar Eu–Eu distances within the chains.

The Au1 and Au2 atoms have coordination number 11 in a very similar manner. They have eight Au, mixed occupied Au/In, and In neighbors besides three coordinating europium atoms. At first sight, the coor-

dination of Au4 seems to be similar, however, the coordination number is reduced to ten. The Au3 atoms have the most irregular coordination in the Eu$_5$Au$_{17.7}$-In$_{4.3}$ structure with four gold, one indium, and five europium atoms in their coordination shell.

The mixed-occupied sites Au5/In3 and In2/Au6 both have coordination number 10. Eight gold neighbors coordinate to these sites in the form of truncated pyramids (distorted cubes) which are capped by indium atoms or the mixed-occupied site. A similar coordination geometry is observed for the indium atoms; however, one capping atom is now europium.

At first sight, the large unit cell and the structure with comparatively low symmetry look quite complex, but one can explain the structure with smaller building units. As emphasized in Fig. 2, we can divide the Eu$_5$Au$_{17.7}$In$_{4.3}$ structure into two different building units. In the middle of the unit cell we observe the motif of distorted hexagonal Au$_6$ prisms which are penetrated by the europium zig-zag chains as discussed above. These structural slabs alternate with slabs containing units of edge-sharing gold tetrahedra. The latter are charge-balanced and separated by further europium atoms. Such Au$_4$ tetrahedra have also been observed in the structures of K$_4$Au$_7$Ge$_2$ [24] and EuAu$_5$ [23] (Fig. 2).

The Au–Au distances within the gold substructure vary between 278 and 300 pm. They are comparable to that in the Au–Au zig-zag chains in EuAu$_3$-
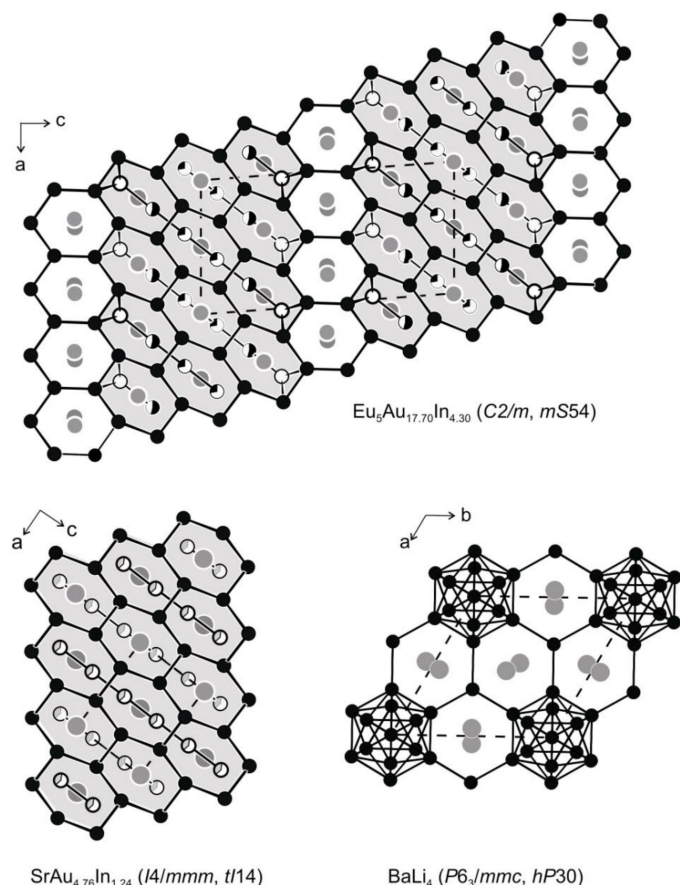
Eu$_5$Au$_{17.70}$In$_{4.30}$ (*C2/m, mS*54)

SrAu$_{4.76}$In$_{1.24}$ (*I4/mmm, tI*14)

BaLi$_4$ (*P6$_3$/mmc, hP*30)

Fig. 3. The crystal structures of Eu$_5$Au$_{17.7}$In$_{4.3}$, SrAu$_{4.76}$In$_{1.24}$ [14] and BaLi$_4$ [25]. The europium (alkaline earth), gold (lithium) and indium atoms are drawn as medium grey, black filled and open circles, respectively. Related structural slabs are shaded. For details see text. Mixed occupied sites are drawn with segments.

In$_3$ (279 pm) [4] and *fcc* gold (288 pm Au–Au) [21], and one can therefore assume significant bonding. The Au–In distances range from 283 to 309 pm. The shorter ones compare well with the sum of the covalent radii [13] of 284 pm, and they are in a range similar to those of the other europium gold indides [4, 6, 11, 12].

In Fig. 3 we present views of the Eu$_5$Au$_{17.7}$In$_{4.3}$ and SrAu$_{4.76}$In$_{1.24}$ [14] structures. Due to the high gold content, both structures display a variety of Au–Au interactions, and one can emphasize a tesselation of different Au$_6$ hexagons. Only elongated hexagons occur in the SrAu$_{4.76}$In$_{1.24}$ [14] structure, while such slabs are interrupted by rows of almost regular hexagons in Eu$_5$Au$_{17.7}$In$_{4.3}$. The latter structural fragment reminds of the BaLi$_4$ structure [25], and consequently one can describe the Eu$_5$Au$_{17.7}$In$_{4.3}$ type as an intergrowth variant of SrAu$_{4.76}$In$_{1.24}$- [14] and BaLi$_4$- [25] related slabs (Fig. 3). In the case of ternary indides, a BaLi$_4$-related structure has been observed for the ordered indide Ca$_3$Ni$_8$In$_4$ [26], a non-centrosymmetric

superstructure variant with Lu$_3$Co$_{7.77}$Sn$_4$-type structure [27].

Finally we comment on the europium valence in the Eu$_5$Au$_{17.7}$In$_{4.3}$ structure. Since we have not obtained a completely X-ray-pure sample, we could not reliably determine the europium valence *via* magnetic susceptibility measurements or [151]Eu Mössbauer spectroscopy. However, the comparison of the europium coordinations and the Eu–Au / Eu–In distances with the data of the compounds EuAu$_3$In$_3$ [4], EuAuIn [6], Eu$_2$Au$_3$In$_4$ [11], and EuAuIn$_2$ [12] with divalent europium, and the structural slabs that occur in these compounds undoubtedly point to divalent europium also in Eu$_5$Au$_{17.7}$In$_{4.3}$.

[1] R. Pöttgen, D. Johrendt, *Chem. Mater.* **2000**, *12*, 875.

[2] R. Pöttgen, *J. Mater. Chem.* **1995**, *5*, 505.

[3] R. Pöttgen, R.-D. Hoffmann, R. Müllmann, B. D. Mosel, G. Kotzyba, *Chem. Eur. J.* **1997**, *3*, 1852.

[4] I. R. Muts, F. M. Schappacher, W. Hermes, V. I. Zaremba, R. Pöttgen, *J. Solid State Chem.* **2007**, *180*, 2202.

[5] D. Kußmann, R. Pöttgen, U. Ch. Rodewald, C. Rosenhahn, B. D. Mosel, G. Kotzyba, B. Künnen, *Z. Naturforsch.* **1999**, *54b*, 1155.

[6] R. Pöttgen, *J. Mater. Chem.* **1996**, *6*, 63.

[7] I. Felner, *J. Phys. Chem. Solids* **1975**, *36*, 1063.

[8] M. M. Abd-Elmeguid, Ch. Sauer, U. Köbler, W. Zinn, J. Röhler, K. Keulerz, *J. Magn. Magn. Mater.* **1985**, *47&48*, 417.

[9] Ch. Sauer, G. Galinski, W. Zinn, M. M. Abd-Elmeguid, *Solid State Commun.* **1987**, *62*, 265.

[10] D. Johrendt, C. Felser, C. Huhnt, G. Michels, W. Schäfer, A. Mewis, *J. Alloys Compd.* **1997**, *241*, 21.

[11] R.-D. Hoffmann, R. Pöttgen, C. Rosenhahn, B. D. Mosel, B. Künnen, G. Kotzyba, *J. Solid State Chem.* **1999**, *145*, 283.

[12] R.-D. Hoffmann, R. Pöttgen, V. I. Zaremba, Ya. M. Kalychak, *Z. Naturforsch.* **2000**, *55b*, 834.

[13] J. Emsley, *The Elements*, Oxford University Press, Oxford **1999**.

[14] I. Muts, S. F. Matar, U. Ch. Rodewald, V. I. Zaremba, R. Pöttgen, *Z. Naturforsch.* **2011**, *66b*, 993.

[15] I. Muts, U. Ch. Rodewald, V. I. Zaremba, R. Pöttgen, *Z. Naturforsch.* **2011**, *66b*, 1101.

[16] R. Pöttgen, Th. Gulden, A. Simon, *GIT Labor-Fachzeitschrift* **1999**, *43*, 133.

[17] R. Pöttgen, A. Lang, R.-D. Hoffmann, B. Künnen, G. Kotzyba, R. Müllmann, B. D. Mosel, C. Rosenhahn, *Z. Kristallogr.* **1999**, *214*, 143.

[18] K. Yvon, W. Jeitschko, E. Parthé, *J. Appl. Crystallogr.* **1977**, *10*, 73.

[19] G. M. Sheldrick, SHELXS-97, Program for the Solution of Crystal Structures, University of Göttingen, Göttingen (Germany). See also: G. M. Sheldrick, *Acta Crystallogr.* **1990**, *A46*, 467.

[20] G. M. Sheldrick, SHELXL-97, Program for the Refinement of Crystal Structures, University of Göttingen, Göttingen (Germany) **1997**. See also: G. M. Sheldrick, *Acta Crystallogr.* **2008**, *A64*, 112.

[21] J. Donohue, *The Structures of the Elements*, Wiley, New York (U. S. A.) **1974**.

[22] A. Iandelli, A. Palenzona, *J. Less-Common Met.* **1968**, *15*, 273.

[23] A. Palenzona, *J. Less-Common Met.* **1984**, *100*, 135.

[24] U. Zachwieja, *Z. Anorg. Allg. Chem.* **1995**, *621*, 975.

[25] F. E. Wang, F. A. Kanda, C. F. Miskell, A. J. King, *Acta Crystallogr.* **1965**, *18*, 24.

[26] V. I. Zaremba, I. R. Muts, Ya. M. Kalychak, R.-D. Hoffmann, R. Pöttgen, *J. Solid State Chem.* **2001**, *160*, 415.

[27] R. Skolozdra, B. Garcia-Landa, D. Fruchart, D. Gignoux, J. L. Soubeyroux, L. G. Akselrud, *J. Alloys Compd.* **1996**, *235*, 210.